PHYSICAL REVIEW A **86**, 011603(R) (2012)

Quantum walk of two interacting bosons

Yoav Lahini, Mor Verbin, Sebastian D. Huber, Yaron Bromberg, Rami Pugatch, and Yaron Silberberg
Department of Physics, Weizmann Institute of Science, Rehovot, Israel
(Received 11 June 2011; published 16 July 2012)

We study the effect of interactions on the propagation of quantum correlations in the bosonic two-body quantum walk. The combined effect of interactions and Hanbury Brown–Twiss interference results in unique spatial correlations which depend on the strength of the interaction, but not on its sign. We experimentally measure the weak interaction limit of these effects using light propagating in a highly nonlinear photonic lattices. Finally, we propose an experimental approach to observe the strong interaction limit using few atoms in optical lattices.

DOI: 10.1103/PhysRevA.86.011603 PACS number(s): 03.75.Lm, 42.50.Ar, 42.65.Tg

Introduction. Understanding highly correlated many-body systems remains both an experimental and theoretical challenge. While there is a rather good understanding of weakly interacting systems, problems involving strong interactions are in general harder to address.

Recently a new approach to the study of quantum dynamics became experimentally accessible through the study of quantum walks (QWs) in lattice potentials [1]. Quantum walks are the quantum counterparts of classical random walks on a discrete lattice: A quantum particle is initially placed at a particular site of a lattice and then tunnels to neighboring sites with equal probability amplitude (see Fig. 1). This basic "step" is repeated, but in contrast to the classical case, quantum mechanical interference leads to distinctively different dynamics. For example, in periodic lattices the wave-function width grows ballistically, while in the classical case the expansion is diffusive.

QWs have received increasing attention due to their relation to various physical and biophysical processes [1–3], and their possible use for quantum computation algorithms [4]. Theoretically, QWs were studied for the single-particle case [1]. Initial experiments studied the physics of single particles by using either classical waves [5], single photons [6,7], or single atoms [8,9]. Moving from one to two noninteracting particles it has recently been shown that indistinguishable quantum walkers can develop nontrivial correlations due to Hanbury Brown–Twiss (HBT) interferences [10–13]. Yet, very little is known of the effect of interactions on the dynamics of the few-body QW [14]. As new systems emerge that can accommodate such experiments [8,9], a systematic study of this problem starting at small particle numbers may offer a "bottom up" approach in the general strive to unders dynamical quantum many-body systems.

In this Rapid Communication we study the effect of interparticle interactions on the two-particle quantum walk and the resulting spatial correlation. We consider two bosons, each initially localized on a single lattice site, undergoing a QW simultaneously (see Fig. 1). We find that the interplay between interactions and quantum two-particle (HBT) interference results in a continuous transition from bosonic to fermionlike spatial correlations between the particles. Interestingly, the correlations depend on the strength of the interaction but not on whether it is attractive or repulsive. We explain the observed correlations by calculating the two-particle spectrum, and interpret our results in light of the physics of attractively and repulsively bound pairs [15,16]. We then present an experimental observation of the weak interaction limit of these effects in nonlinear photonic lattices, by using an experimental implementation of the truncated Winger approximation [17,18]. Finally, we outline an experimental approach to observe the strong interaction limit using a small number of atoms carefully positioned in optical lattices.

QW of two interacting particles. We start by calculating the QW of two interacting particles. We consider the one-dimensional Bose-Hubbard model

$$H = -J \sum_{\langle l,m \rangle} a_l^\dagger a_m + \frac{U}{2} \sum_m \hat{n}_m(\hat{n}_m - 1), \qquad (1)$$

where $a_m^\dagger$ (a_m) is the creation (annihilation) operator for a particle at site m, $\hat{n}_m = a_m^\dagger a_m$ is the corresponding number operator, J is the tunneling amplitude between nearest neighbors, and U is the on-site interaction energy which can be attractive (negative) or repulsive (positive). (See Fig. 1.)

We study the QW of two indistinguishable particles, each initially localized on a single site in a periodic lattice. We consider two different initial conditions: one in which the two particles are localized at adjacent lattice sites $|\psi_{\text{initial}}\rangle = a_1^\dagger a_0^\dagger |0\rangle$, and a second in which the particles are initially placed at the same site, $|\psi_{\text{initial}}\rangle = (a_0^\dagger)^2|0\rangle$. Our focus lies on the particle density $n_r(t)=\langle a_r^\dagger a_r\rangle$ and on the two-particle correlation $\Gamma_{q,r}(t) = \langle a_q^\dagger a_r^\dagger a_r a_q\rangle$ which are calculated after an

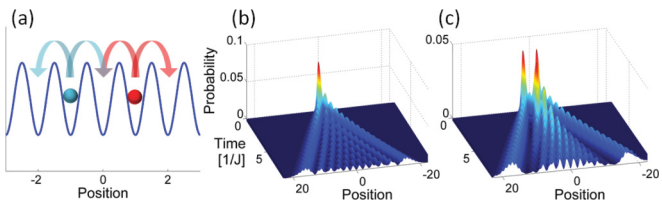

FIG. 1. (Color online) Two-particle quantum walk. (a) An illustration of two identical atoms initially placed on two sites of an optical lattice, and allowed to tunnel to neighboring sites and interfere. (b) The evolution of the particle density plotted against position (in lattice sites) for the case of a single-atom quantum walk. (c) The evolution of the density for a two-atom quantum walk. This density is only weakly affected by interactions, while the two-particle correlations are strongly modified.

evolution time T for different values of the interaction U. At all stages the particles are far from the lattice boundaries.

The results for $U = 0$ correspond to the results reported in Refs. [10,11]: When two non-interacting bosons start the QW at the same site, after propagation each particle can be found on either side of the site of origin, reflected in the four symmetric peaks in the correlation matrix inset for Fig. 2(a). When the particles are initially placed at adjacent sites, HBT interference results in spatial bunching, and the two particles propagate together either to the left side of the distribution [peak at the bottom left corner of the correlation matrix in Fig. 2(g)] or to the right (top right corner). Other initial conditions, in which the particles are further separated in space, result in more complicated correlation patterns [10]. Such initial states and the results of interactions will be discussed in the Supplemental Material [19].

Let us now turn to the discussion of interaction effects. Figures 2(b)–2(e) show the results for increasing repulsive interaction U for in the case of two bosons initially localized at the same site. The spatial correlations show that as $|U|$ increases the two particles tend to propagate as a pair, while the density distribution becomes localized. Figures 2(g)–2(l) show the results for the case in which the particles are initially placed at different sites, $|\psi_{\text{initial}}\rangle = a_1^\dagger a_0^\dagger|0\rangle$. Here, the particle density depends only weakly on U, but the two-particle correlation undergoes a fundamental change: The spatial bunching effects which occur in the noninteracting case gradually transform to spatial antibunching [Fig. 2(k)]. For large values of the interaction strength $|U|$, the correlation between the two bosons becomes very similar to the correlation exhibited by two noninteracting fermions, prepared in the same initial configuration [compare Figs. 2(k) and 2(l)]. The noninteracting fermionic and the interacting bosonic matrices become identical at the limit of $|U| \to \infty$, while the density becomes identical to the one for $U = 0$. An interesting result is that in both cases the effect of interactions does not depend on the sign of U; it is identical for both attractive and repulsive interactions. We note that for initial conditions in which the two particles are further separated in space, interactions also drive the system towards fermionlike correlations, only that now they have a more complicated spatial structure—see the Supplemental Material [19] for additional experimental and theoretical results.

The two-particle spectrum. To understand these results we consider the two-particle spectrum of the system, as shown in Fig. 3 for two particles on a lattice with $M = 29$ sites. Each of the two-particle eigenfunctions can be written as $\Psi(r_1,r_2)$, where r_1 and r_2 are the positions of the two particles on the lattice. Introducing the center-of-mass coordinate $R = (r_1 + r_2)/2$ and the relative coordinate $r = r_1 - r_2$, we can solve the Schrödinger equation with the ansatz $\Psi(r_1,r_2) = \exp(iKR)\psi_K(r)$, where K is the quasimomentum of the center-of-mass motion and $\psi_K(r)$ is the pair wave function [16].

For finite interaction strengths, the spectrum separates into two bands. The main part of the spectrum, containing $[M(M-1)]/2$ eigenstates, consists of scattering states having low probability at $r = 0$, whose energy is given by the noninteracting part of the Hamiltonian in Eq. (1). The smaller

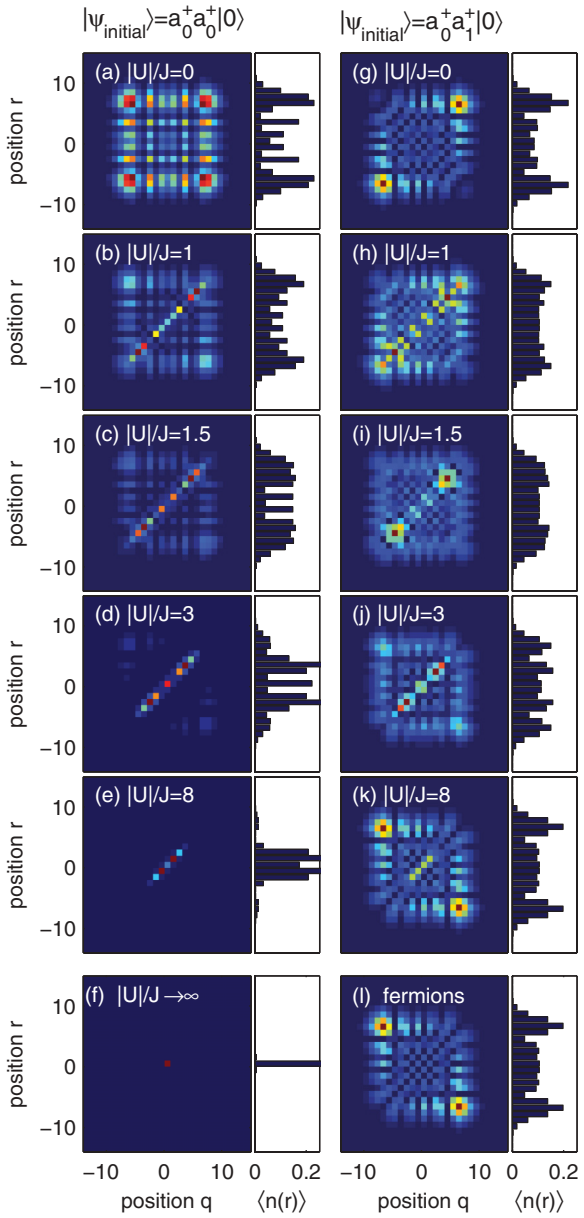

FIG. 2. (Color online) Two-particle correlations for interacting quantum walkers. Left column: Correlations after propagation time $T = 4$ in units of $1/J$, where initially the two particles are placed at the same site, $|\psi_{\text{initial}}\rangle = (a_0^\dagger)^2|0\rangle$. The correlations are plotted against the positions of the two particles q and r, in lattice sites away from the origin. (a) For zero interactions, the particles show no interference in the correlations [10]. (b)–(f) As the interaction is increased, the correlations show the formation of bound pairs, while the density distribution (shown on the right-hand side of each plot) becomes increasingly localized. Right column: Similar results for an initial condition in which the two particles are placed at adjacent sites $|\psi_{\text{initial}}\rangle = a_1^\dagger a_0^\dagger|0\rangle$. (g) At $U = 0$ the correlation shows spatial bunching. (h)–(j) The correlations change as the interaction $|U|$ is increased, while the density is only weakly affected. (k) At strong interactions the correlation is transformed to spatial antibunching, similar to the correlation that would be exhibited by two noninteracting fermions initially placed in the same configuration (l). All results are identical for both attractive and repulsive interactions.

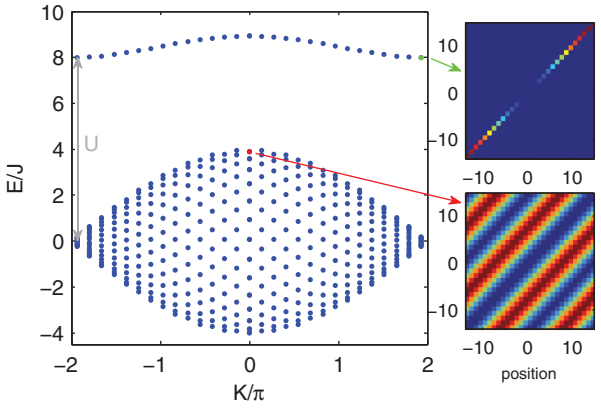

FIG. 3. (Color online) Spectrum and two-particle eigenmodes of Eq. (1) for $U = 8$. The spectrum is separated into two minibands. The higher band consists of bound pair states in which the two particles only occupy the same sites (nonzero values mainly on the diagonal $r = q$, top inset), while the lower band consists of states in which the two particles have small probability to occupy the same site (lower inset). The gap is proportional to the interaction strength U. Attractive interactions $U < 0$ yield an identical yet inverted spectrum. The position axis in the insets is given in lattice sites.

part of the spectrum (M eigenstates) consists of states $\psi_K^{\rm bs}(r)$ which have a large probability for two particles to occupy the same site, i.e., $|\psi_K^{\rm bs}(0)|^2 \to 1$ ($U \to \infty$) [16] (see the insets in Fig. 3). This miniband has higher or lower energies than the main part of the spectrum, depending on the sign of the interaction; nevertheless, the spatial probability distribution of the two-particle eigenstates is identical.

Using this picture, it is possible to explain the results in Fig. 2. An initial state in which the two particles occupy the same site with strong attractive or repulsive interaction will mostly contain two-particle states from the smaller miniband. As a result, the two particles will remain bound, as described by Winkler *et al.* in Ref. [15] [see Figs. 2(g)–2(l)]. A complementary process happens if the particles initially occupy different sites. This initial condition excites mainly scattering states from the main part of the spectrum. As a result, the particles have low probability to be found at the same site throughout the evolution, and will not show bunching.

Let us now turn to the case of strong interactions $|U| \gg J$. Our goal is to understand the "fermionization" as observed in the correlator $\Gamma_{q,r}(t)$ for an initial state in which the particles are found at different sites. We start by noting that by focusing on the scattering states we can describe the Hamiltonian (1) using hard-core bosons, where doubly occupied sites are eliminated from the Hilbert space. Formally we replace the bosonic operators with spin-1/2 operators: $a_m^\dagger \to S_m^+$, $a_m \to S_m^-$.

Next, we use a standard mapping from spin-1/2 to fermionic operators $f_m, f_m^\dagger$ [20]. Let us review the essential steps of this mapping to understand the "fermionic" behavior of $\Gamma_{q,r}(t)$. Spin-1/2 and fermionic operators share the local property $(f_m^\dagger)^2 = f_m^2 = (S_m^+)^2 = (S_m^-)^2 = 0$. However, spins on different sites commute, whereas fermions pick up a minus sign. In the sought mapping one corrects for this via the Jordan-Wigner string $\exp(i\phi_m)$:

$$S_m^- = e^{-i\phi_m} f_m, \quad S_m^+ = e^{i\phi_m} f_m^\dagger,$$

with

$$\phi_m = \pi \sum_{l=1}^{m-1} f_l^\dagger f_l.$$

It is now straightforward to check that for $\Gamma_{q,r}(t)$ the Jordan-Wigner string drops out. Hence, the correlations for hard-core bosons are identical to the ones obtained for noninteracting fermions in accordance with our observation in Fig. 2.

Experimental results. In this section we experimentally observe the semiclassical limit of the effects described above in a nonlinear optical setup. We do so by experimentally implementing the truncated Wigner approximation (TWA) [17,18]. The TWA is an approximate semiclassical method to calculate the time evolution of an given initial state in an interacting many-body system. The essence of the TWA is to use a classical Hamiltonian to evolve a family of initial conditions which in turn are distributed according to the Wigner distribution of the chosen initial quantum state.

In the case described here, the initial state describes two particles localized on different sites. The Wigner distribution of this initial state resembles a ring in the number-phase plane. The number is well defined but the phase is wildly fluctuating [18]. However, its Wigner distribution has both positive and negative values. This is a common problem in TWA as one has to interpret it as a probability. Usually this is accounted for by approximating the exact Wigner distribution with the closest purely positive function.

The experimental setup that was used to implement the TWA is the nonlinear waveguide lattice [21]. The dynamics of light in these systems has been shown to be well described by

$$H = -J \sum_{\langle l,m \rangle} \Psi_l^* \Psi_m + \gamma \sum_m |\Psi_m|^4, \tag{2}$$

which is just the classical version of Eq. (1). Here Ψ_i describes the amplitude of the light field at site i. We approximate the actual Wigner distribution with two coherent states, each initially placed on single lattice sites. In each realization, the phase between the two states was random (to account for a different position on the Wigner distribution). When averaged over all the phases this reproduces the best approximation to the actual Wigner distribution.

In the experiments we have used two laser beams (that act as our two coherent states), each initially injected into a single waveguide in the lattice. In each realization, the phase between the two lasers was randomized (to account for a different position on the Wigner distribution). We propagated the two beams through the waveguide lattice, measured the intensity-intensity correlation function, and averaged over all the results. The only approximation we make is that we ignore the cases in which the Wigner distribution is negative.

Indeed, in the experiments described below, we find that in the limit of weak interactions the measured classical correlations for nonlinear waves are similar to the predicted quantum correlations.

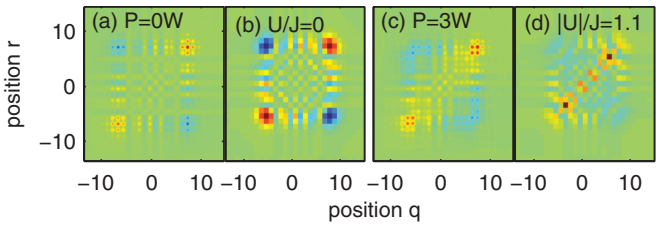

FIG. 4. (Color online) Experimental measurements of the fluctuation in intensity correlations for nonlinear thermal light. (a) The fluctuations in the intensity correlations in the linear case, when two thermal beams are injected into two adjacent sites, corresponding to $|\psi_{\text{initial}}\rangle = a_1^\dagger a_0^\dagger |0\rangle$. The results show spatial bunching [10]. (b) The predictions of the quantum theory for two noninteracting particles initially placed at the same locations. (c) Experimental results for nonlinear thermal waves. (d) The predictions of the quantum theory for two interacting particles. Note the similarity between the classical results and the quantum prediction in both cases. Positions are given in lattice sites.

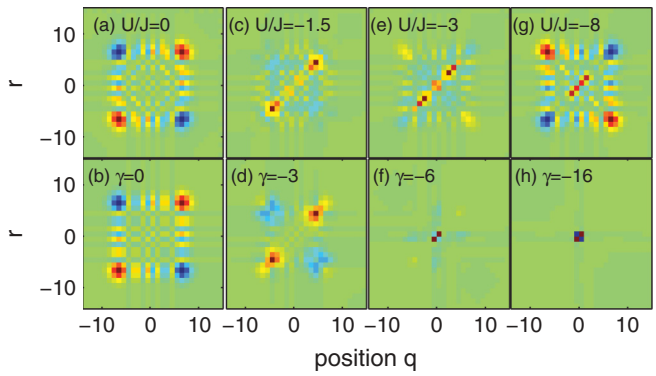

FIG. 5. (Color online) Simulations comparing the fluctuations for the quantum (top panel) and the classical (bottom) cases, with increasing $|U|$ or nonlinear coefficient $|\gamma|$, correspondingly, for $|\psi_{\text{initial}}\rangle = a_1^\dagger a_0^\dagger |0\rangle$. The two sets of results look similar for weak interactions (a)–(d). However, beyond $|U| = 1.5$ (e)–(h) the two results diverge—the quantum correlations transform to fermioniclike correlations, while the classical correlations become increasingly localized. In all cases the positions are given in lattice sites.

In Fig. 4 we present experimental measurements of intensity correlations obtained with $|\psi_{\text{initial}}\rangle = a_1^\dagger a_0^\dagger |0\rangle$. Numerical results are presented in Fig. 5. In all figures we compare the correlation fluctuations $\Gamma^F_{q,r}(t) = \langle a_q^\dagger a_r^\dagger a_r a_q\rangle - \frac{1}{2}\langle a_q^\dagger a_q\rangle \cdot \langle a_r^\dagger a_r\rangle = \Gamma_{q,r} - \frac{1}{2} n_q \cdot n_r$, which are a better basis for comparison between the quantum and classical (thermal) case. As the results show, for weak interactions the classical correlations follow the quantum predictions [see Figs. 4 and 5(a)–5(d)]. However, as interactions become stronger, the two systems diverge—while the quantum system exhibits a switch to fermionlike correlations, the classical system cannot follow, and remains with modified, localized correlations, as in Figs. 5(e)–5(h).

Proposed cold-atom experiment. Experimentally, the strong interaction limit of the effects discussed above can be observed using techniques that recently became available. The experimental requirements include the ability to (i) initially localize exactly two quantum particles at two predetermined lattice sites, (ii) to allow these particles to freely tunnel and exhibit a QW, (iii) to control the interaction strength (or the interaction-to-tunneling ratio), and (iv) to image single particles in the lattice sites after some evolution time. An example of a system that can accommodate such experiments was recently presented in Ref. [9]. In this system, the authors placed single atoms at selected sites and allowed them to tunnel, exhibiting, on the ensemble average, the dynamics of continuous-time QWs [1,5]. Using a similar approach, we propose starting with an ensemble of two (and in principle N) atoms separated by several sites. The density after time T can be measured in the same manner as in Ref. [9], and the two (or N) particle correlations can be directly assessed from the raw data. An important aspect will be the ability to control interactions, for example, via tuning a Feshbach resonance, or controlling the ratio U/J. For the two-particle case and at zero interactions, the results should correspond to those presented in Ref. [10] and observed in Ref. [11] using photon pairs. However, when interactions will be introduced we predict the results presented above: If the particles are placed one on top of each other, they will tunnel as a pair [15], and the density will become localized. If they are placed at different, not too distant sites, the density will show only minor changes as a function of U, but the two-particle correlation will change significantly, reaching a fermionlike correlation at the limit of strong interactions. In the same spirit, this system can be used to directly measure the dynamic properties and correlations for large numbers of particles, a problem which quickly becomes impossible to compute.

Conclusions. The approach presented here offers a path to study highly correlated quantum systems by considering the dynamical behavior of an increasing number of particles, each initially confined to a single site. Such dynamics can be experimentally explored in systems such as described in Ref. [9]. As the number of particles increases, the problem will become uncomputable, but experimentally accessible. It would be of special interest to study these effects in disordered potentials.

[1] J. Kempe, Contemp. Phys. **44**, 307 (2003).
[2] G. S. Engel *et al.*, Nature (London) **446**, 782 (2007).
[3] T. Kitagawa, M. S. Rudner, E. Berg, and E. Demler, Phys. Rev. A **82**, 033429 (2010).
[4] A. M. Childs, Phys. Rev. Lett. **102**, 180501 (2009).
[5] H. B. Perets *et al.*, Phys. Rev. Lett. **100**, 170506 (2008).
[6] A. Schreiber *et al.*, Phys. Rev. Lett. **104**, 050502 (2010).
[7] M. A. Broome *et al.*, Phys. Rev. Lett. **104**, 153602 (2010).

[8] M. Karski *et al*., Science **325**, 174 (2009).
[9] C. Weitenberg *et al*., Nature (London) **471**, 319 (2011).
[10] Y. Bromberg, Y. Lahini, R. Morandotti, and Y. Silberberg, Phys. Rev. Lett. **102**, 253904 (2009).
[11] A. Peruzzo *et al*., Science **329**, 1500 (2010).
[12] K. Mayer *et al*., Phys. Rev. A **83**, 062307 (2011).
[13] R. Hanbury Brown and R. Q. Twiss, Nature (London) **177**, 27 (1956).
[14] M. Stefanak *et al*., New J. Phys. **13**, 033029 (2011).
[15] K. Winkler *et al*., Nature (London) **441**, 853 (2006).
[16] P. F. Maldague, Phys. Rev. B **16**, 2436 (1977).
[17] A. PolkovnikovAnn. Phys. **325**, 1790 (2010).
[18] A. Polkovnikov, Phys. Rev. A **68**, 033609 (2003); **68**, 053604 (2003).
[19] See Supplemental Material at http://link.aps.org/supplemental/10.1103/PhysRevA.86.011603 for additional theoretical and experimental results for particles initially placed at non-adjacent sites.
[20] P. Jordan and E. Wigner, Z. Phys. **47**, 631 (1928).
[21] D. N. Christodoulides, F. Lederer, and Y. Silberberg, Nature (London) **424**, 817 (2003); F. Lederer *et al*., Phys. Rep. **463**, 1 (2008).